

Cardiac myocyte-specific HIF-1 α deletion alters vascularization, energy availability, calcium flux, and contractility in the normoxic heart

Yan Huang,* Reed P. Hickey,* Jennifer L. Yeh,* Dinggang Liu,* Agnes Dadak,[†] Lawrence H. Young,* Randall S. Johnson,[†] and Frank J. Giordano*

*Department of Medicine, Yale University, New Haven, Connecticut; [†]Department of Biology, University of California, San Diego

Corresponding author: Frank J. Giordano, BCMM 436C, 295 Congress Ave., New Haven, CT 06510. E-mail: Frank.Giordano@yale.edu

ABSTRACT

At a resting pulse rate the heart consumes almost twice-as much oxygen per gram tissue as the brain and more than 43 times more than resting skeletal muscle (1). Unlike skeletal muscle, cardiac muscle cannot sustain anaerobic metabolism. Balancing oxygen demand with availability is crucial to cardiac function and survival, and regulated gene expression is a critical element of maintaining this balance. We investigated the role of the hypoxia-inducible transcription factor HIF-1 α in maintaining this balance under normoxic conditions. Cardiac myocyte-specific HIF-1 α gene deletion in the hearts of genetically engineered mice caused reductions in contractility, vascularization, high-energy phosphate content, and lactate production. This was accompanied by altered calcium flux and altered expression of genes involved in calcium handling, angiogenesis, and glucose metabolism. These findings support a central role for HIF-1 α in coordinating energy availability and utilization in the heart and have implications for disease states in which cardiac oxygen delivery is impaired.

Heart muscle requires a constant supply of oxygen. When oxygen supply does not match myocardial demand cardiac contractile dysfunction occurs, and prolongation of this mismatch leads to apoptosis and necrosis. Coordination of oxygen supply and myocardial demand involves immediate adaptations, such as coronary vasodilatation, and longer-term adaptations that include altered patterns of gene expression (2–4). How the expression of multiple genes is coordinated with oxygen availability in the heart and the impact of oxygen-dependent gene expression on cardiac function are insufficiently understood. Further elucidating these relationships may help clarify the molecular pathology of various cardiovascular disease states, including ischemic cardiomyopathy and myocardial hibernation (5, 6).

Key words: hypoxia • cardiac muscle • contraction • gene expression

The hypoxia-inducible transcription factor HIF-1 α represents a major pathway controlling gene expression in response to oxygen levels (7–9). HIF-1 α is a basic helix–loop–helix protein that forms a dimer with the aryl hydrocarbon receptor nuclear translocator

(ARNT) and binds a core response element in a growing repertoire of HIF-responsive genes. These include genes involved in angiogenesis, glucose metabolism, vasomotor control, and erythropoiesis, many of which are involved in either the delivery of oxygen and nutrients to cells or controlling cellular utilization of these substrates (8, 10). The biologic importance of HIF-1 α has been documented recently in such diverse settings as cartilage morphogenesis and cutaneous inflammation (11, 12). Although best identified with transcriptional activation in response to hypoxia, mounting evidence suggests that HIF-1 α plays an important role regulating gene expression during normoxia and that this can have an important effect on various basal cellular functions (13). ATP levels, for example, are decreased in normoxic fibroblasts null for HIF-1 α , and glycolysis is abnormal in HIF-1 α null chondrocytes under aerobic conditions, thus documenting the substantive role of HIF-1 α in the transcriptional regulation of basal cellular metabolism (13, 14). In the heart where oxygen demand can vary considerably in response to alterations in heart rate, contractility, and hemodynamic load, the HIF-1 α oxygen-sensing transcriptional control pathway may be of particular importance.

HIF-1 α expression is increased in the myocardium of patients with ischemic heart disease, which suggests an important role for HIF-1 α in cardiac adaptation to chronic ischemia (15). Global deletion of HIF-1 α results in embryonic lethality with failure of neural tube closure, defective vascularization, and increased thickness of the embryonic heart (16, 17). Although HIF-1 α regulates VEGF expression, the cardiac phenotype of global HIF null mice is quite distinct from global VEGF null mice in which a thin-walled myocardium develops (18). It is also distinct from the dilated thin-walled hearts we have described previously in cardiac myocyte-specific VEGF null mice (19), which suggests effects of HIF-1 α in the heart beyond those attributable to regulation of VEGF expression alone. As a “master switch” coordinating gene expression with oxygen availability, the up-regulation of HIF-1 α in ischemic human hearts strongly suggests a major role for HIF-1 α in the heart. In addition, the ability of HIF-1 α to induce therapeutic angiogenesis is currently being studied in patients with advanced ischemic heart disease and peripheral arterial disease (20). Further understanding of the role played by HIF-1 α in the heart is, therefore, of significant clinical importance. To investigate this we used a cre-lox approach to generate mice with cardiac myocyte-specific deletion of HIF-1 α .

MATERIALS AND METHODS

Generation of cardiac myocyte HIF-1 α null mice

Our HIF-1 α floxed-allele mice, in which lox-P sites bracket exon 2, have no basal phenotype and have been described previously (21). To generate mice with cardiac myocyte-specific deletion of HIF-1 α , the floxed-allele mice were crossed with MLC2v-Cre mice in which cre recombinase expression is driven by the MLC2v promoter. Both strains of mice were backcrossed into a C57B6 background for multiple generations. The MLC2v-Cre mice were generated by “knocking-in” cre in the endogenous MLC2v locus. These mice, which have also been extensively studied and described previously, did not have a basal phenotype as a haploid genotype and drove cre expression specifically in cardiac myocytes of the left ventricle (19, 22). For all experiments and group comparisons cardiac HIF-1 α null mice were MLC2v-Cre +/- and HIF-1 α loxP +/+, and controls were HIF-1 α lox P +/+ cre negative littermates.

Hemodynamic and echocardiography studies

Anesthesia was induced by intramuscular ketamine injection. Mice were then intubated, placed on positive pressure ventilation and light anesthesia maintained by inhaled isoflurane. The right common jugular vein was cannulated with polyethylene tubing and a 1.9 French transducer-tipped catheter (Millar Inc., Houston, TX) was advanced into the left ventricle via the right carotid artery. Left ventricular pressures, including high-fidelity positive and negative dP/dt, were measured under basal conditions and during intravenous infusion of graduated doses of dobutamine. Data were recorded by using MacLab software and were analyzed by using the Heartbeat program (UC San Diego; 19). Echocardiograms were obtained on lightly anesthetized mice (isoflurane inhalation via nosecone) by using a 15 Mhz transducer and a Sonos 7500 console. Zoomed 2D images were used to determine a short axis plane at the level of the papillary muscles and then M-mode was obtained at this level. Measurements were obtained using the 7500 analysis software.

Single cell shortening and fluorescent calcium transients

Cardiac myocytes were isolated from HIF-1 α null and control hearts by a described previously retrograde aortic coronary perfusion method (19). Briefly, the aorta was cannulated in situ after which the heart was rapidly excised and washed in ice-cold saline. The heart was then hung on a modified Langendorf apparatus and a buffered solution containing Type II collagenase was perfused through the coronary bed. After the heart became flaccid it was minced with fine scissors and further digestion was performed in solution. The final digest was passed through a fine filter, and the cardiac myocytes were placed in calcium-free Tyrodes solution. Calcium was replaced by gradual titration into the Tyrodes solution. The cells were then placed in a Petri dish invested with platinum electrodes and placed on the heated stage of a Zeiss Axiovert 135 inverted microscope fitted with a Delta Scan Photometry system (Photon Technology International, Inc.) for measurement of calcium transients. A video edge detection system (Crescent Electronics) measured the magnitude of cell shortening. For these studies the cells were paced at a rate of 12 Hz. Fluo-3 (Molecular Probes, San Diego, CA) was loaded into myocytes according to the manufacturer's recommendations and was used as an indicator of cytosolic calcium. We captured calcium transients using Felix software (Photon Technology International, Inc, Lawrenceville, NJ) and background subtracted. The time for intracellular calcium to decrease to 50% of maximum amplitude ($t_{1/2}[\text{Ca}^{2+}]_{in}$) was determined as described previously (23). Percentage of cell shortening was expressed as $([\text{basal length}-\text{contracted length}]/\text{basal length}) \times 100$.

Gene expression and floxing efficiency

For gene expression studies, total RNA was extracted from the left ventricles of cardiac HIF-1 α null and littermate control mice using RNA Stat-60TM reagent (Tel-Test, Inc, Friendswood, TX). RNA was treated with Rnase-free DNase I (Roche, Basel, Switzerland) and column-purified (Qiagen, Inc., Valencia, CA). RT-PCR was performed in two steps. First-strand cDNA was synthesized with ProSTARTM First-Strand RT-PCR kit (Stratagene, LaJolla, CA) using random primers. Conditions for the RT reactions were 1 h at 42°C, 10 min at 95°C. SYBR Green JumpStartTM Taq ReadyMix (Sigma, St. Louis, MO) was used in the second step of real-time PCR amplification of first-strand cDNA. We ran reactions in 96-well plates on an Opticon 2

Real-Time quantitative PCR block (MJ Research, Inc., Waltham, MA). For all primer pairs the presence of a single gene product was verified by agarose gel electrophoresis. Melting curves were also examined after each run. Primer sequences used include Vegf-A forward AAGGAGAGCAGAAGTCCCATGA, reverse CACAGGACGGCTTGAAGATGT; GLUT-1 forward GGGCTGCCAGGTTCTAGTC, reverse CCTCCGAGGTCCTTCTCA; GLUT-4 forward TATTTGGCTTTGTGGCCTTC, reverse CGGCAAATACAAGGAAGACG; LDH forward GCTTCGATTACCCCTGTGA, reverse GTCGGCCTAGGCTGTTTG; PGK forward CAAATTTGATGAGAATGCCAAGACT, reverse TTCTTGCTGCTCTCAGTACCACA; SERCA2a forward TCCATGAGCAAGATGTTTGTGAA, reverse TCCCGAATGACAGACATAATCTTCT; PLB forward CGATCACCGAAGCCAAGGTCTC, reverse GTGGCGGCAGCTCTTCACAGA; 18 s rRNA forward TTCCGATAACGAACGAGACTCT, reverse TGGCTGAACGCCACTTGTC.

For Western blot analysis, equally loaded protein samples underwent electrophoresis on 10% NuPAGE gels (Invitrogen, San Diego, CA). Protein bands were transferred onto nitrocellulose membranes and blocked with 5% nonfat milk. Membranes were incubated at 4°C overnight with primary antibody (anti-SERCA2a, anti-phospholamban, anti-GLUT-1; Santa Cruz Biotechnology, Santa Cruz, CA), washed, and incubated for 1 h with secondary antibody and developed by using chemiluminescence. For determination of floxing efficiency, genomic DNA was isolated from cardiac myocytes and non-myocytes isolated from knockout and control hearts. Quantitative PCR was performed by using a primer pair designed to give product only in the absence of floxing.

ATP, phosphocreatine, and lactate analysis

Left ventricular heart samples were harvested from cardiac HIF-1 α null and littermate controls by rapid freeze-clamp method. Samples were rapidly homogenized in 5% trichloroacetic acid (TCA) in a mechanical shear homogenizer (PowerGen 125, Model TH115/FTH115) and were centrifuged at 10,000 g for 5 min at 4°C. These supernatants were used for all subsequent assays. Quantification of ATP and lactate content was accomplished by using standard commercial biochemical assays as described previously (Sigma Diagnostics; 24, 25). Phosphocreatine was measured by mixing supernatant to 0.2M Tris assay buffer containing 0.1M MgCl₂ and 1% NADP at a final pH of 7.5. and by calculating from the change in measured optical density (340 dA) after addition of 5 mM/ml ADP and creatine kinase (26).

Histology and vessel counts

For standard histology, hearts were fixed in formalin, embedded in paraffin, sectioned, and stained (H&E, lipid-O red, trichrome) by the Yale Pathology core facility. For immunohistochemistry OTC-embedded frozen sections were used. Sections (5 μ m) were cut and fixed with acetone/methanol. A monoclonal anti-PECAM antibody (Invitrogen) was used for microvessel counts and an anti-smooth muscle actin antibody (R&D Systems, Minneapolis, MN) was used for assessing smooth muscle invested vessels. Three HIF null and 3 control hearts were sectioned, and digital images from 5 separate 40 \times fields were obtained from each section. Vessel counts were determined from the digital images by two separate blinded investigators. Vessel density was corroborated by Western blot for PECAM on protein lysates from HIF null and control hearts. For electron microscopy (EM), hearts were fixed by retrograde perfusion with a

buffered solution containing 2% EM grade glutaraldehyde. Subsequent processing was performed in the Yale EM core.

RESULTS

Cardiac HIF-1 α null mice are viable but exhibit cardiac contractile dysfunction and prolonged cardiomyocyte calcium transients

Homozygous cardiac myocyte-specific deletion of HIF-1 α resulted in normal litter sizes with expected genotype frequencies. This is in contradistinction to global homozygous deletion of HIF-1 α that results in embryonic lethality (9, 16, 17). MLC2v-Cre-mediated HIF-1 α gene deletion was specific and efficient in cardiac myocytes, with an ~90% gene deletion frequency by real-time quantitative PCR (Fig. 1a-c). This value is similar to MLC2v-mediated floxing efficiency we have described previously in the heart by Southern blot (19). Cardiac HIF-1 α null mice tended to have lower body weights than age- and gender-matched littermate controls, but this difference was not significant (Fig. 1d). Histologic and electron microscopic analysis of HIF-1 α null hearts did not reveal fibrosis, myocyte loss, lipid accumulation, or apparent ultra-structural abnormalities (Fig. 1 and data not shown).

Cardiac contractility was assessed in vivo by invasive hemodynamic analysis and echocardiography and in vitro by measuring cell shortening in isolated cardiac myocytes. In vivo assessment of age- and gender-matched HIF-1 α deletion, and littermate control mice revealed significant decreases in +dP/dt and -dP/dt in the cardiac HIF-1 α null mice at baseline and in response to progressive adrenergic stimulation, which suggests both systolic and diastolic dysfunction secondary to loss of HIF-1 α (Fig. 2a, b). Isovolumic relaxation time (tau) was increased in the HIF-1 α null hearts as further evidence of diastolic dysfunction (Fig. 2e). Heart rates, peak pressures, and left ventricular end-diastolic pressures were not statistically different at baseline or during dobutamine infusion, which suggests that the contractile abnormalities noted were intrinsic to the myocardium and not secondary to alterations in loading conditions or the force-frequency relationship (Fig. 2c, d, f). Non-invasive assessment by echocardiography demonstrated a significant reduction in fractional shortening, providing further in vivo evidence of contractile dysfunction ($26.1 \pm 1.1\%$ HIF null, $n=25$, vs. $33.2 \pm 1.4\%$ control, $n=28$; $P<0.001$; Fig. 2g).

To investigate whether the contractile dysfunction documented in cardiac HIF-1 α null mice is caused by a primary defect in cardiomyocyte contractility or an indirect effect such as reduced myocardial vascularity, cell shortening was measured in isolated HIF-1 α null and control cardiomyocytes during electrical stimulation at 12 Hz. Cell shortening was reduced from $11.60 \pm 1.42\%$ of resting length in control cells to $4.95 \pm 0.80\%$ in HIF-1 α null cardiomyocytes ($P<0.001$; Fig. 3a), indicating an intrinsic defect in cardiac myocyte contractility in the absence of HIF. To determine whether alterations in the rate of calcium reuptake from the cytosol contribute to the diastolic dysfunction of HIF-1 α null hearts, we performed photometric analysis of dynamic calcium flux. HIF-1 α null cells demonstrated a prolongation in the time required to reduce cytosolic calcium to 1/2 maximum amplitude ($t_{1/2} [Ca^{++}]_{in}$; HIF-1 α null = 0.195 ± 0.001 s vs. control = 0.169 ± 0.001 s; $P<0.001$; $n=3$ mice per group, 10 cells analyzed /mouse, 10 data points/cell; Fig. 3b-c), suggesting that the diastolic dysfunction noted in HIF-1 α null hearts is

partially attributable to a defect in cytosolic calcium lowering during cell relaxation. Evaluation of SERCA2 protein levels revealed a significant reduction in SERCA2 expression in the left ventricle of the HIF-1 α null hearts ([Fig. 3d](#)), suggesting that reduction of this critical sarcoplasmic reticulum calcium pump may contribute to the slowing of calcium reuptake noted in HIF null cardiomyocytes.

Cardiac deletion of HIF-1 α causes mild hypovascularity and hypertrophy

Although HIF-1 α is an upstream transcriptional mediator of several angiogenesis-associated genes, including vascular endothelial growth factor (VEGF), the relative role of HIF-1 α in defining cardiac vascularity has remained unclear. Deletion of HIF-1 α in cardiac myocytes resulted in a $15.6 \pm 6.18\%$ average reduction of vessel counts in the left ventricles of cardiac HIF-1 α null mice compared with controls ($P < 0.05$; $n = 3$ mice per group, 10 separate fields per heart; [Fig. 4a–c](#)), which suggests an important though not exclusive role for HIF-1 α in defining basal cardiac vascularity during normoxia. These findings correlated with anti-PECAM Western blots obtained from HIF null and control hearts ($n = 3$ /group; [Fig. 4d](#)). There were no changes in the number of smooth muscle invested vessels ([Fig. 4e](#)), which suggests a more important role for HIF-1 α in defining the microvasculature than larger blood vessels.

To determine the effect of cardiac HIF-1 α deletion and associated hypovascularity on left ventricular (LV) mass, LV to body weight (BW) ratios were determined. Deletion of HIF-1 α in the LV myocardium resulted in an increase in LV/BW ratios from 2.70 ± 0.10 mg/g in control littermates to 3.09 ± 0.07 in cardiac HIF-1 α null mice ($n = 9$ per group; $P < 0.001$; [Fig. 4f](#)), which is consistent with mild cardiac hypertrophy. Cardiac ultrasound analysis correlated with this finding and demonstrated significant increases in the diastolic thickness of both the intraventricular septum (IVSd) and the posterior wall (PWd; [Fig. 4g, h](#)). Interestingly, the left ventricular end-diastolic diameter (LVEDD) was significantly reduced in HIF-1 α null hearts ([Fig. 4i](#)), hence the loss of cardiomyocyte-specific HIF-1 α leads to thicker hearts with smaller LV chambers. Thus, in contradistinction to the cardiac VEGF null phenotype we have previously reported, LV mass is preserved in cardiac HIF-1 α null mice, despite concomitant hypovascularity (19).

HIF-1 α is a significant determinant of basal gene expression in the normoxic heart. Although best known as a transcriptional mediator of altered gene expression during hypoxia, there is accumulating evidence that HIF-1 α plays an important role under normoxic conditions (13, 14). To investigate the role of HIF-1 α in determining gene expression in the normoxic heart the expression of a panel of representative genes was assessed by real-time quantitative RT-PCR. Cardiac myocyte-specific deletion of HIF-1 α resulted in significantly reduced basal expression of selected genes involved in angiogenesis, glucose transport, glycolysis, and calcium handling, including vascular endothelial growth factor (VEGF-A), the glucose transporter Glut-1, phosphoglycerate kinase (PGK), lactate dehydrogenase (LDH), and the sarcoplasmic reticulum calcium pump SERCA2 ([Fig. 5](#)). There was no concomitant reduction of phospholamban (PLB) or Glut-4. Although cardiac myocytes represent less than 1/3 of total cells in the heart, total HIF-1 α mRNA in the cardiac myocyte HIF-1 α null hearts was reduced to 23% of control hearts, thus demonstrating limited or no compensatory expression of HIF-1 α in alternative cell types in the heart. There was a trend toward a small increase in expression of HIF-2 α that did not reach

significance. Interestingly, expression of endothelin-1, a HIF-1 α responsive gene, was increased nearly twofold in HIF-1 α null hearts (Fig. 5), suggesting either an alternative mechanism of ET-1 gene regulation in cardiac myocytes or increased ET-1 expression from non-myocytes in response to HIF-1 α deletion in the cardiac myocyte population. Platelet derived growth factor (PDGF), a HIF-1 α responsive angiogenic gene, was also increased in the HIF-1 α null hearts, again suggesting complex regulation or a non-cardiomyocyte source.

Cardiac HIF-1 α deletion results in reduced myocardial ATP, phosphocreatine, and lactate levels

Given the established role of HIF-1 α as a transcriptional mediator of several genes associated with energy metabolism and glycolysis, the effects of cardiac HIF-1 α deletion on cardiac content of ATP, phosphocreatine, and lactate was investigated. The HIF-1 α null hearts demonstrated a $29.5 \pm 5.6\%$ ($P \leq 0.05$) reduction in ATP content and a $23.8 \pm 2.1\%$ decrease in lactate levels ($P \leq 0.05$) when compared with littermate controls (Fig. 6a, b). Phosphocreatine content was similarly decreased in the absence of HIF ($15.2 \pm 3.3\%$ HIF-1 α null hearts vs littermate control hearts; $P \leq 0.05$; Fig. 6c). These changes were evident in normoxic hearts without stress provocation and reflect the basal high-energy phosphate content of these hearts in the presence and absence of HIF-1 α . The decreased expression of Glut-1 documented at the mRNA level was corroborated at the protein level by Western blot (Fig. 6d), further supporting the possibility that altered glucose transport contributes to the reduction in high-energy phosphates observed.

DISCUSSION

Here we show that loss of the HIF-1 α transcriptional control pathway in cardiac muscle alters gene expression and has deleterious effects on cardiac function, vascularity, energy availability, and calcium handling. These effects occur without the provocation of induced hypoxia or ischemia and establish that in cardiac muscle transcriptional control by HIF-1 α is required during normoxia. In the heart, therefore, HIF-1 α appears to act as an oxygen-sensing transcriptional modifier that coordinates gene expression at all oxygen levels, not just in response to hypoxia or ischemia.

The mechanism of reduced contractility in HIF-1 α null hearts in vivo is likely multifactorial, including the effects of hypovascularity, altered energy metabolism, and anomalous calcium handling. That isolated HIF-1 α null cardiac myocytes demonstrate reduced contractility at the single cell level establishes that the observed in vivo contractile dysfunction is not entirely due to the concomitant decrease in vascularity. Previously we have shown that cardiac myocyte specific deletion of VEGF-A results in reduced coronary vascularity and concomitant cardiac contractile dysfunction (19). It would therefore be reasonable to attribute the phenotype of HIF-1 α null hearts to the loss of HIF-1 α -mediated VEGF-A transcriptional activation. The phenotype of the HIF-1 α null hearts is, however, quite distinct from that of the thin-walled dilated VEGF null hearts, establishing that the effects of HIF-1 α deletion are not fully attributable to loss of VEGF-A transcription alone. Nonetheless, there is a decrease in myocardial vessel counts at the microvascular level establishing that HIF-1 α is indeed required for normal coronary vascularization. This reduction, corroborated by reduced PECAM levels in the myocardium, is relatively small and suggests that compensatory and/or alternative pathways are defining

coronary vascularization. Interestingly, although VEGF-A mRNA is markedly reduced in the HIF-1 α null hearts VEGF-C expression is unchanged, this finding is consistent with previous reports demonstrating the lack of VEGF-C response to hypoxia (27). Platelet-derived growth factor (PDGF) levels are moderately increased in HIF-1 α null hearts despite previous documentation that PDGF is HIF-1 α responsive (28). This finding suggests either that HIF-1 α regulation of PDGF is redundant with other pathways, and/or that loss of HIF-1 α -induced PDGF expression from cardiac myocytes is compensated by PDGF expression by the vasculature or other cell types.

Altered sarcoplasmic reticulum calcium re-uptake secondary to decreased expression of SERCA2 could also be contributing to the observed contractile dysfunction. Single cell calcium studies revealed a prolongation of calcium reuptake consistent with what is generally seen with decreased SERCA2 function. Alterations in sarcoplasmic reticulum calcium handling can adversely effect both diastolic and systolic function (29) as was seen in the HIF-1 α null hearts. The mechanism leading to decreased SERCA2 mRNA in HIF-1 α null hearts is unclear. There are putative HIF-1 α binding sites in the SERCA2 regulatory region, but promoter studies in vitro with a 3.5 Kb 5' fragment of the SERCA2 regulatory region demonstrated only minimal induction of transcription by HIF-1 α (unpublished data; Giordano lab). Although this does not rule out loss of SERCA2 transcriptional activation by HIF-1 α as a contributory mechanism, it suggests that there are additional pathways involved.

Relative SERCA2 mRNA levels have been shown to be decreased in hypertrophied and failing hearts, although no single definitive signaling pathway has been established to explain this phenomenon (30, 31). Interestingly, unlike the thin-walled dilated hearts that occur secondary to cardiac VEGF-A deletion, HIF-1 α null hearts demonstrate increased wall thickness and HW/BW ratios (19). The mechanism of this mild hypertrophy is unclear, especially in the face of hypovascularization, but it is consistent with the gross developmental cardiac phenotype noted in the global homozygous HIF-1 α null mice that die in utero (16). Possible contributory mechanisms include hypertrophy secondary to endothelin 1 (ET-1), which was increased twofold in the HIF-1 α null hearts, or an adaptive response to altered glucose metabolism, similar to the gross hypertrophy noted in Glut-4 deficient hearts (32). We and others have previously shown that protein kinase C activation leads to a decrease in relative SERCA2 mRNA levels (33, 34). Although the cardiac response to ET-1 is complex and includes an acute positive inotropic effect, ET-1 activates PKC, has been associated with relative decreases in SERCA2, and ET-1 receptor blockade rescues reduced SERCA2 levels and improves heart failure (35, 36). This does not establish an etiologic role for ET-1 in the cardiac HIF-1 α null phenotype, and certainly the increased expression of ET-1 may be a secondary event. It is interesting that ET-1 is increased in HIF-1 α null hearts because ET-1 has been demonstrated to be a HIF-1 α responsive gene (37). In this study the cell type of origin was not determined for ET-1 and it is possible that the increase in ET-1 mRNA observed was from non-myocytes in the heart.

Also interesting is that the HIF null hearts have reduced LV chamber diameters. Myocardial oxygen consumption (MVO₂) is proportional to myocardial wall tension (WT), and in accordance with a modified version of the Law of LaPlace $WT \sim rP/2\pi$: where r = the radius of the LV; p = pressure within the LV, and π = wall thickness. Thus, the morphometry of the HIF null hearts should result in lower cardiac MVO₂, a potential benefit in the setting of defective

energy metabolism or nutrient delivery resulting from loss of HIF-1 α -mediated transcriptional effects. Whether the altered cardiac morphometry in HIF-1 α null hearts is adaptive or an epiphenomenon is unclear, but the possibility that HIF-1 α may act as a bridge between oxygen and nutrient availability and cardiac morphometry is intriguing.

The critical importance of glucose transport and the glycolytic machinery in the heart is now well established (32, 38, 39). Cardiac-specific deletion of GLUT-4, for example, results in cardiac hypertrophy and both a greater sensitivity to and inability to recover from ischemia (32, 38). HIF-1 α is a transcriptional regulator of GLUT-1 expression as well as that of most of the glycolytic enzymes. We found reductions in the expression of GLUT-1 and of representative glycolytic enzymes in the HIF-1 α null hearts, along with reductions in high-energy phosphate and lactate content. Sarcolemmal translocation of glucose transporters was not assessed in this study, however there was no compensatory increase in myocardial GLUT-4 gene expression. Whether the reduction in high-energy phosphate content is directly related to decreased expression of GLUT-1 and the glycolytic enzymes that are known to be HIF-1 α responsive, or whether the reduction involves other metabolism-related genes not yet identified as HIF-1 α responsive, is unclear. What appears clear is that HIF-1 α plays a critical role in defining cardiac energetics, even under normoxic conditions. We hypothesize that HIF-1 α acts in part as a myocardial “thermostat”, adapting the expression of genes involved in oxygen delivery, energy delivery, and energy metabolism to the chronic workload of the heart. More in-depth analysis of the alterations in glucose and fatty acid metabolism that occur in the absence of myocardial HIF-1 α expression will be required to more fully define the role of HIF-1 α as a transcriptional regulator of cardiac energy metabolism.

In summary, these studies establish that cardiac myocyte-specific HIF-1 α expression is required for basal transcriptional activation of multiple genes in the heart during normoxia and that myocardial gene expression is oxygen-sensitive at physiologic oxygen levels. Loss of this basal HIF-1 α mediated transcriptional activation has deleterious effects on cardiac function, energetics, and vascularization, and these findings provide clear evidence that in the heart HIF-1 α plays an important role under normal physiologic conditions. Although not addressed in this study, HIF-1 α likely plays an even more important role in conditions of cardiac stress, such as ischemia and pressure overload. Further elucidation of the role of HIF-1 α in cardiomyocyte biology may give significant insight into cardiovascular disease states characterized by chronic or recurrent reductions in myocardial oxygen tension and perhaps identify new targets for therapeutic intervention.

ACKNOWLEDGMENTS

The authors would like to thank William Sessa for helpful review and comments on the manuscript, and Raymond Russell for advice on measuring high-energy phosphates in the heart. This work was funded by National Institutes of Health RO1 HL64001 to F.J.G.

REFERENCES

1. West, J. B. (1991) *Physiologic Basis of Medical Practice*. Williams and Wilkins: Baltimore: Baltimore, MD

2. Simkhovich, B. Z., Marjoram, P., Poizat, C., Kedes, L., and Kloner, R. A. (2003) Brief episode of ischemia activates protective genetic program in rat heart: a gene chip study. *Cardiovasc. Res.* **59**, 450–459
3. Simkhovich, B. Z., Kloner, R. A., Poizat, C., Marjoram, P., and Kedes, L. H. (2003) Gene expression profiling—a new approach in the study of myocardial ischemia. *Cardiovasc. Pathol.* **12**, 180–185
4. Lyn, D., Liu, X., Bennett, N. A., and Emmett, N. L. (2000) Gene expression profile in mouse myocardium after ischemia. *Physiol. Genomics* **2**, 93–100
5. Anversa, P., and Sonnenblick, E. H. (1990) Ischemic cardiomyopathy: pathophysiologic mechanisms. *Prog. Cardiovasc. Dis.* **33**, 49–70
6. Kloner, R. A., Bolli, R., Marban, E., Reinlib, L., and Braunwald, E. (1998) Medical and cellular implications of stunning, hibernation, and preconditioning: an NHLBI workshop. *Circulation* **97**, 1848–1867
7. Wang, G. L., Jiang, B. H., Rue, E. A., and Semenza, G. L. (1995) Hypoxia-inducible factor 1 is a basic-helix-loop-helix-PAS heterodimer regulated by cellular O₂ tension. *Proc. Natl. Acad. Sci. USA* **92**, 5510–5514
8. Giordano, F. J., and Johnson, R. S. (2001) Angiogenesis: the role of the microenvironment in flipping the switch. *Curr. Opin. Genet. Dev.* **11**, 35–40
9. Carmeliet, P., Dor, Y., Herbert, J. M., Fukumura, D., Brusselmans, K., Dewerchin, M., Neeman, M., Bono, F., Abramovitch, R., Maxwell, P., et al. (1998) Role of HIF-1alpha in hypoxia-mediated apoptosis, cell proliferation and tumour angiogenesis. *Nature* **394**, 485–490
10. Semenza, G. L. (2001) Hypoxia-inducible factor 1: control of oxygen homeostasis in health and disease. *Pediatr. Res.* **49**, 614–617
11. Cramer, T., and Johnson, R. S. (2003) A novel role for the hypoxia inducible transcription factor HIF-1alpha: critical regulation of inflammatory cell function. *Cell Cycle* **2**, 192–193
12. Schipani, E., Ryan, H. E., Didrickson, S., Kobayashi, T., Knight, M., and Johnson, R. S. (2001) Hypoxia in cartilage: HIF-1alpha is essential for chondrocyte growth arrest and survival. *Genes Dev.* **15**, 2865–2876
13. Pfander, D., Cramer, T., Schipani, E., and Johnson, R. S. (2003) HIF-1alpha controls extracellular matrix synthesis by epiphyseal chondrocytes. *J. Cell Sci.* **116**, 1819–1826
14. Seagroves, T. N., Ryan, H. E., Lu, H., Wouters, B. G., Knapp, M., Thibault, P., Laderoute, K., and Johnson, R. S. (2001) Transcription factor HIF-1 is a necessary mediator of the pasteur effect in mammalian cells. *Mol. Cell. Biol.* **21**, 3436–3444

15. Lee, S. H., Wolf, P. L., Escudero, R., Deutsch, R., Jamieson, S. W., and Thistlethwaite, P. A. (2000) Early expression of angiogenesis factors in acute myocardial ischemia and infarction. *N. Engl. J. Med.* **342**, 626–633
16. Ryan, H. E., Lo, J., and Johnson, R. S. (1998) HIF-1 alpha is required for solid tumor formation and embryonic vascularization. *EMBO J.* **17**, 3005–3015
17. Iyer, N. V., Kotch, L. E., Agani, F., Leung, S. W., Laughner, E., Wenger, R. H., Gassmann, M., Gearhart, J. D., Lawler, A. M., Yu, A. Y., et al. (1998) Cellular and developmental control of O₂ homeostasis by hypoxia-inducible factor 1 alpha. *Genes Dev.* **12**, 149–162
18. Ferrara, N., Carver-Moore, K., Chen, H., Dowd, M., Lu, L., O'Shea, K. S., Powell-Braxton, L., Hillan, K. J., and Moore, M. W. (1996) Heterozygous embryonic lethality induced by targeted inactivation of the VEGF gene. *Nature* **380**, 439–442
19. Giordano, F. J., Gerber, H. P., Williams, S. P., VanBruggen, N., Bunting, S., Ruiz-Lozano, P., Gu, Y., Nath, A. K., Huang, Y., Hickey, R., et al. (2001) A cardiac myocyte vascular endothelial growth factor paracrine pathway is required to maintain cardiac function. *Proc. Natl. Acad. Sci. USA* **98**, 5780–5785
20. Genzyme (2003) HIF-1a gene therapy in bypass patients.
21. Cramer, T. (2003) HIF-1a is Essential for Myeloid Cell-Mediated Inflammation. *Cell* **112**, 645–657
22. Chen, J., Kubalak, S. W., and Chien, K. R. (1998) Ventricular muscle-restricted targeting of the RXRalpha gene reveals a non-cell-autonomous requirement in cardiac chamber morphogenesis. *Development* **125**, 1943–1949
23. Giordano, F. (1996) Adenovirus-mediated overexpression of SERCA2 normalizes SERCA2 levels and calcium transients in phorbol ester-induced cardiac hypertrophy. *Circulation*
24. Cramer, T., Yamanishi, Y., Clausen, B. E., Forster, I., Pawlinski, R., Mackman, N., Haase, V. H., Jaenisch, R., Corr, M., Nizet, V., et al. (2003) HIF-1alpha is essential for myeloid cell-mediated inflammation. *Cell* **112**, 645–657
25. Seagroves, T. N., Hadsell, D., McManaman, J., Palmer, C., Liao, D., McNulty, W., Welm, B., Wagner, K. U., Neville, M., and Johnson, R. S. (2003) HIF1alpha is a critical regulator of secretory differentiation and activation, but not vascular expansion, in the mouse mammary gland. *Development* **130**, 1713–1724
26. Nielsen, J. N., Mustard, K. J., Graham, D. A., Yu, H., MacDonald, C. S., Pilegaard, H., Goodyear, L. J., Hardie, D. G., Richter, E. A., and Wojtaszewski, J. F. (2003) 5'-AMP-activated protein kinase activity and subunit expression in exercise-trained human skeletal muscle. *J. Appl. Physiol.* **94**, 631–641
27. Enholm, B. P.K., Ristimaki, A., Kumar, V., Gunji, Y., Klefstrom, J., Kivinen, L., Laiho, M., Olofsson, B., Joukov, V., Eriksson, U., and Alitalo, K. (1997) Comparison of VEGF,

VEGF-B, VEGF-C, and Ang-1 mRNA regulation by serum, growth factors, oncoproteins, and hypoxia. *Oncogene* **14**, 2475–2483

28. Kelly, B. D., Hackett, S. F., Hirota, K., Oshima, Y., Cai, Z., Berg-Dixon, S., Rowan, A., Yan, Z., Campochiaro, P. A., and Semenza, G. L. (2003) Cell type-specific regulation of angiogenic growth factor gene expression and induction of angiogenesis in nonischemic tissue by a constitutively active form of hypoxia-inducible factor 1. *Circ. Res.* **93**, 1074–1081
29. Periasamy, M., Reed, T. D., Liu, L. H., Ji, Y., Loukianov, E., Paul, R. J., Nieman, M. L., Riddle, T., Duffy, J. J., Doetschman, T., et al. (1999) Impaired cardiac performance in heterozygous mice with a null mutation in the sarco(endo)plasmic reticulum Ca²⁺-ATPase isoform 2 (SERCA2) gene. *J. Biol. Chem.* **274**, 2556–2562
30. Meyer, M., Schillinger, W., Pieske, B., Holubarsch, C., Heilmann, C., Posival, H., Kuwajima, G., Mikoshiba, K., Just, H., Hasenfuss, G., et al. (1995) Alterations of sarcoplasmic reticulum proteins in failing human dilated cardiomyopathy. *Circulation* **92**, 778–784
31. Arai, M., Matsui, H., and Periasamy, M. (1994) Sarcoplasmic reticulum gene expression in cardiac hypertrophy and heart failure. *Circ. Res.* **74**, 555–564
32. Abel, E. D., Kaulbach, H. C., Tian, R., Hopkins, J. C., Duffy, J., Doetschman, T., Minnemann, T., Boers, M. E., Hadro, E., Oberste-Berghaus, C., et al. (1999) Cardiac hypertrophy with preserved contractile function after selective deletion of GLUT4 from the heart. *J. Clin. Invest.* **104**, 1703–1714
33. Hartong, R., Villarreal, F. J., Giordano, F., Hilal-Dandan, R., McDonough, P. M., and Dillmann, W. H. (1996) Phorbol myristate acetate-induced hypertrophy of neonatal rat cardiac myocytes is associated with decreased sarcoplasmic reticulum Ca²⁺ ATPase (SERCA2) gene expression and calcium reuptake. *J. Mol. Cell. Cardiol.* **28**, 2467–2477
34. Porter, M. J., Heidkamp, M. C., Scully, B. T., Patel, N., Martin, J. L., and Samarel, A. M. (2003) Isoenzyme-selective regulation of SERCA2 gene expression by protein kinase C in neonatal rat ventricular myocytes. *Am. J. Physiol. Cell Physiol.* **285**, C39–C47
35. Sakai, S., Miyauchi, T., Kobayashi, M., Yamaguchi, I., Goto, K., and Sugishita, Y. (1996) Inhibition of myocardial endothelin pathway improves long-term survival in heart failure. *Nature* **384**, 353–355
36. Sakai, S., Miyauchi, T., and Yamaguchi, I. (2000) Long-term endothelin receptor antagonist administration improves alterations in expression of various cardiac genes in failing myocardium of rats with heart failure. *Circulation* **101**, 2849–2853
37. Minchenko, A., and Caro, J. (2000) Regulation of endothelin-1 gene expression in human microvascular endothelial cells by hypoxia and cobalt: role of hypoxia responsive element. *Mol. Cell. Biochem.* **208**, 53–62

38. Tian, R., and Abel, E. D. (2001) Responses of GLUT4-deficient hearts to ischemia underscore the importance of glycolysis. *Circulation* **103**, 2961–2966
39. Russell, R. R., III, Bergeron, R., Shulman, G. I., and Young, L. H. (1999) Translocation of myocardial GLUT-4 and increased glucose uptake through activation of AMPK by AICAR. *Am. J. Physiol.* **277**, H643–H649

Received Jan. 7, 2004; accepted March 23, 2004.

Fig. 1

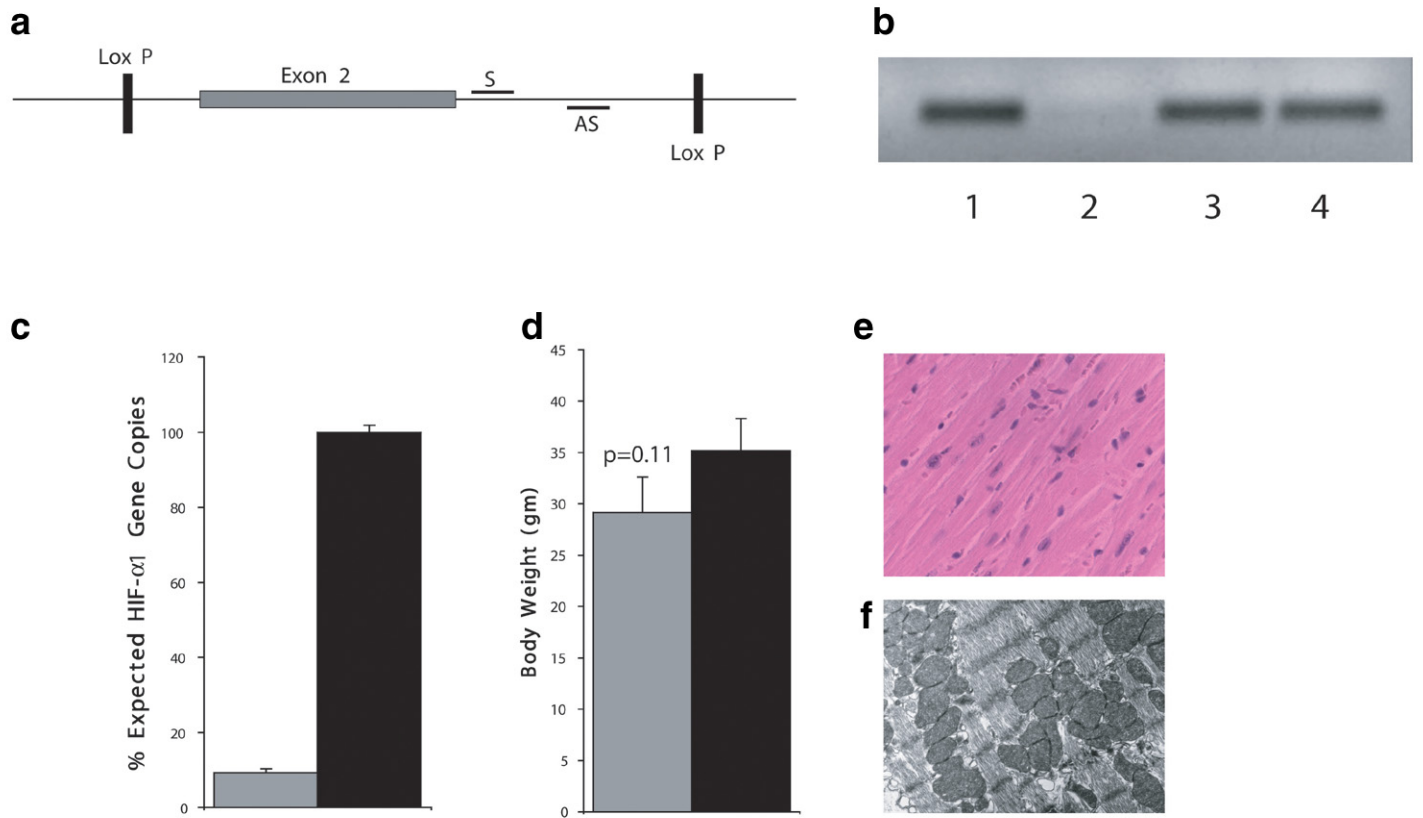


Figure 1. Homozygous deletion of HIF-1 α in cardiac myocytes is non-lethal and does not alter cardiac muscle morphometry or ultrastructure. *a*) Exon 2 of HIF-1 α was excised by Cre-induced recombination in left ventricular cardiac myocytes. Diagram depicts lox P sites and sites at which sense (S) and anti-sense (AS) primers used to determine gene excision frequency bind to genomic DNA. *b*) Genomic DNA from Cre- lox P ^{+/+} cardiac myocytes (Lane 1) and tails (Lane 3), and Cre⁺ lox P ^{+/+} cardiac myocytes (Lane 2) and tails (Lane 4) was amplified by PCR and demonstrates efficient and specific deletion of HIF-1 α in cardiac myocytes. *c*) Real-time quantitative PCR demonstrated a $93 \pm 3\%$ HIF-1 α excision frequency in cardiac myocytes from cardiac HIF-1 α null mice. *d*) Cardiac HIF-1 α null mice demonstrated a trend toward reduced body weights. *e*) Hematoxylin and eosin staining, and transmission electron microscopy (*f*), demonstrated normal myocardial architecture and ultrastructure in the myocardium of HIF-1 α null hearts.

Fig. 2

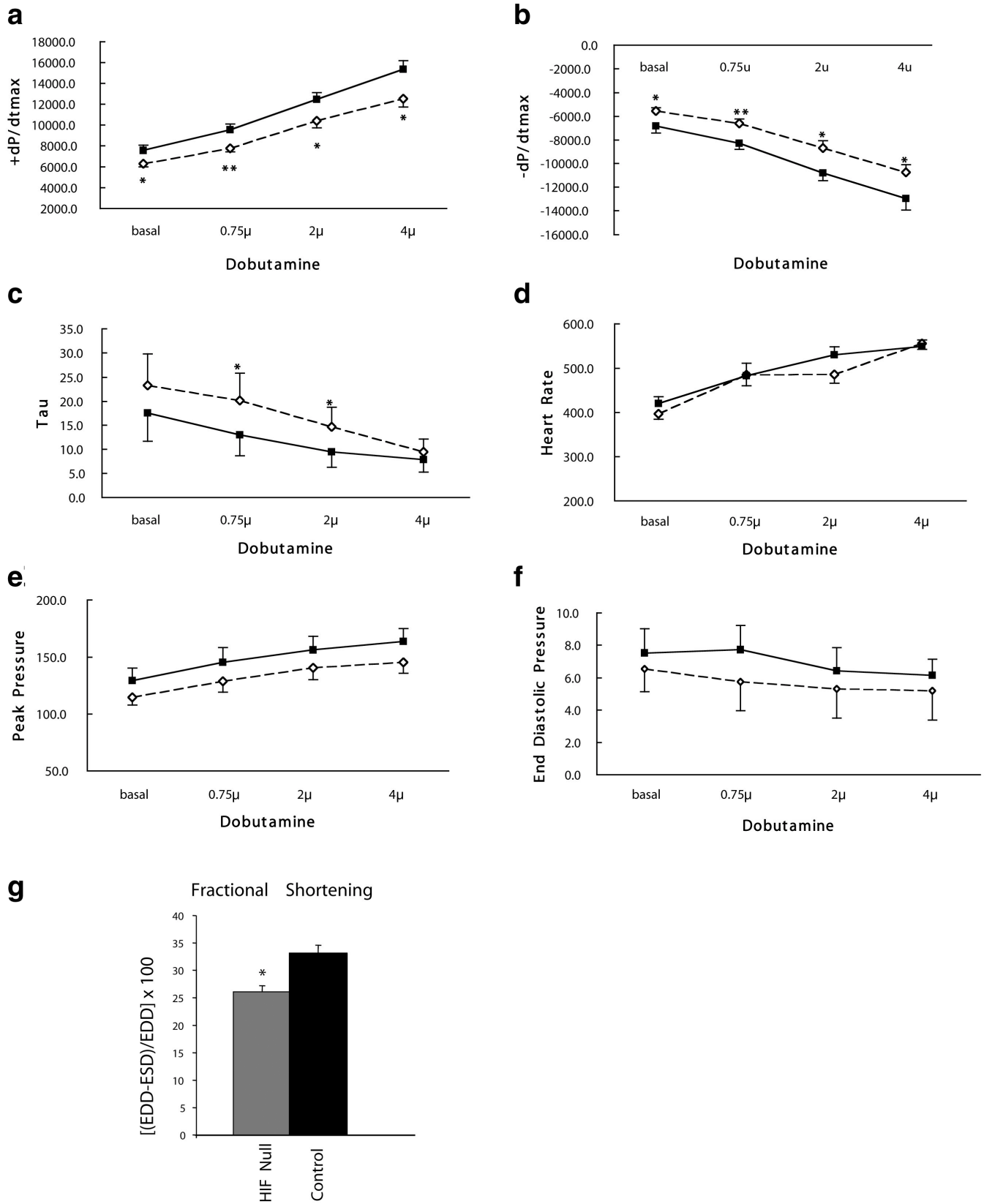


Figure 2. Expression of HIF-1 α in cardiac myocytes is required to maintain normal heart function *in vivo*.

Hemodynamic characteristics were compared between mice in which HIF-1 α was deleted specifically from cardiac myocytes (open symbols; $n=13$) and littermate controls (closed squares; $n=9$). **a–b**) The maximum rates of left ventricular pressure development (+dP/dt) and pressure decline (–dP/dt) were significantly reduced in cardiac HIF-1 α null mice under basal conditions and during adrenergic stimulation with increasing doses of dobutamine. **c**) As further evidence of diastolic dysfunction, isovolumic relaxation time (Tau) was significantly increased at low and moderate levels of dobutamine stimulation, indicating impaired relaxation. **d**) Heart rates were similar in both groups under all conditions. **e, f**) Peak developed pressures tended to be less in the cardiac HIF-1 α mice, and left ventricular end-diastolic pressures tended to be mildly higher, although these difference were not statistically significant for either parameter under any measured conditions. **g**) Echocardiography correlated with the hemodynamic data, revealing reduced fractional shortening in the HIF-1 α null hearts ($n=25$ HIF null, 28 littermate controls). * $P < 0.01$, ** $P < 0.001$; Dobutamine doses are in micrograms/kg body weight/minute.

Fig. 3

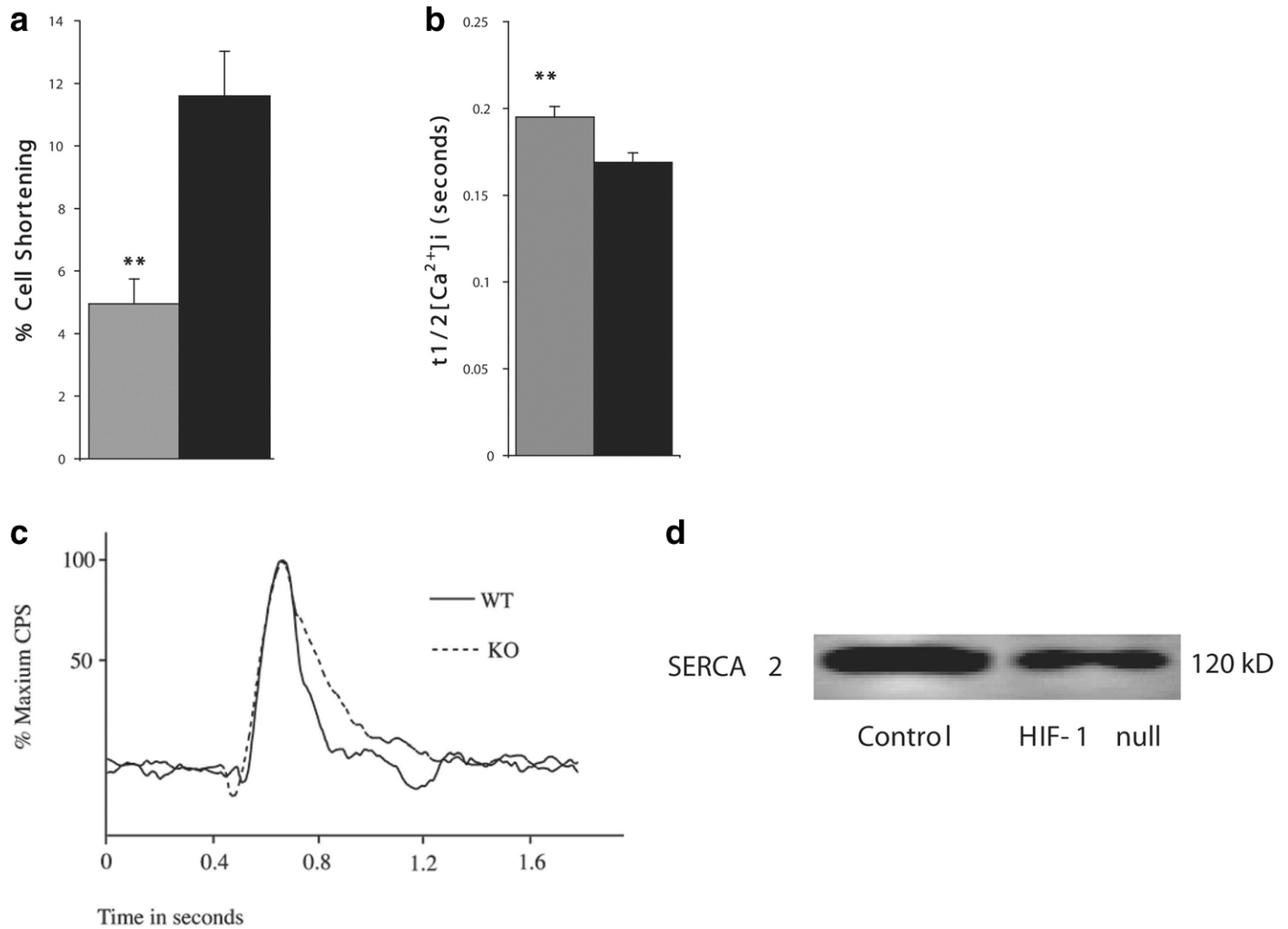


Figure 3. HIF-1 α null cardiac myocytes demonstrate reduced contractility and prolongation of cytosolic calcium lowering. *a*) HIF-1 α null cardiac myocytes (grey bars) demonstrate decreased reduction in length during excitation–contraction induced by constant rate pacing than cells from control littermates. *b–c*) Alterations in single-cell contractility are accompanied by a prolongation in the time to reduce cytosolic calcium to 1/2 maximum after excitation-associated calcium release (t1/2 [Ca²⁺]_i) in HIF-1 α null cells (Fluo-3-based photometry). *d*) Western blotting reveals reduced SERCA2 protein in HIF-1 α null cardiac myocytes. CPS = counts per second (referring to photomultiplier tube counts of light units); WT = control = age/gender matched littermates; KO = HIF-1 α null. ***P*<0.005

Fig. 4

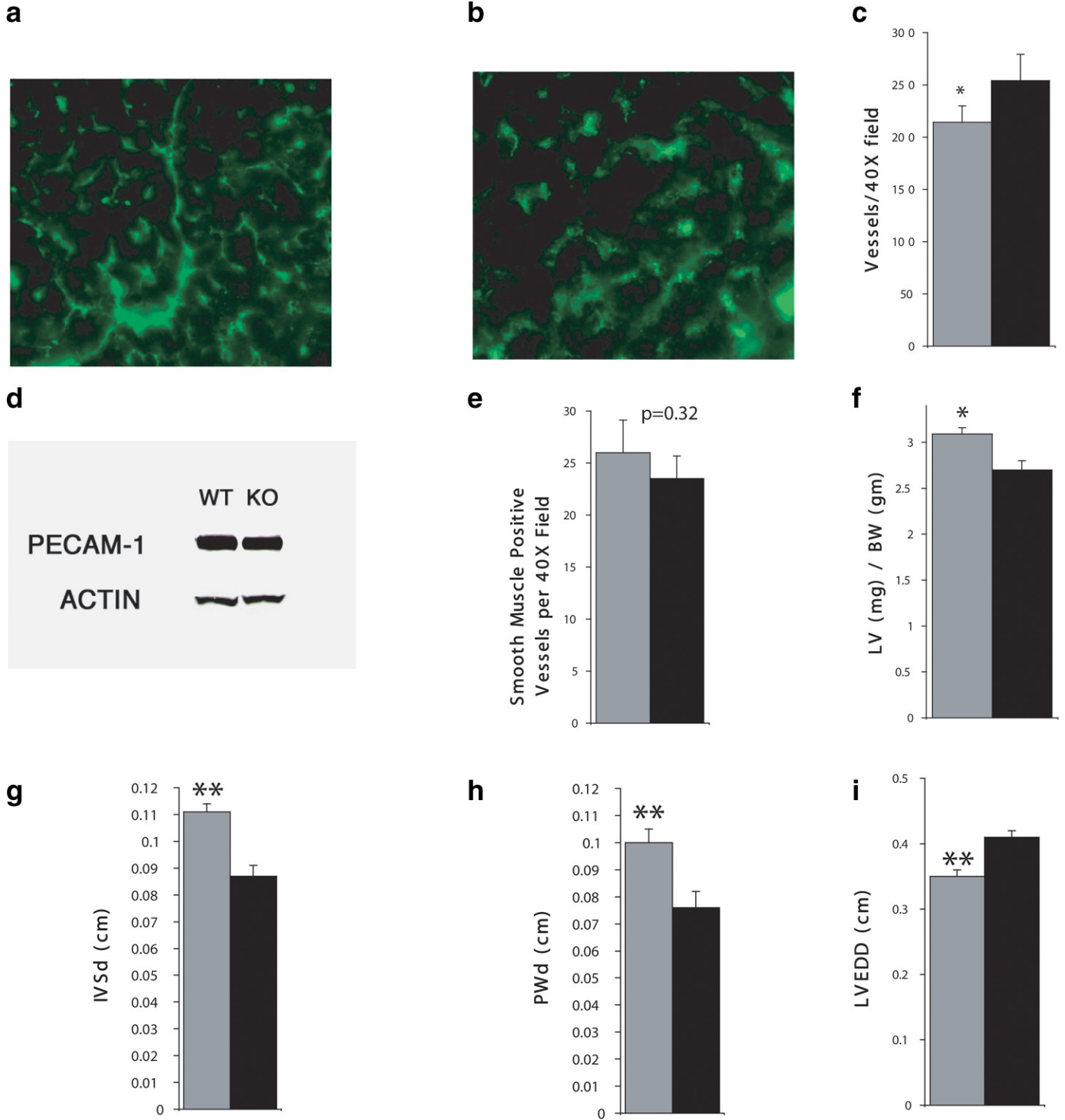


Figure 4. Cardiac myocyte-specific HIF-1 α deletion reduces cardiac vascularity without a concomitant loss of LV mass. Blood vessels in left ventricle myocardium from control mice (*a*) and age/gender-matched cardiac HIF-1 α null littermates (*b*) were fluorescently identified with an antibody against PECAM. Comparative vessel counts are expressed per 40 \times microscopic field and demonstrate a reduction in microvessels in the HIF-1 α null hearts (*c*). These data correlated with PECAM levels determined by Western blot, using muscle-specific actin as a loading standard (*d*). Smooth muscle (SMC) invested vessels were similarly assessed with an anti-SMC actin antibody. Cardiac HIF-1 α null hearts had similar numbers of SMC-invested vessels as controls (*e*), indicating that reduced vascularity in HIF-1 α null hearts is at the microvessel level. Left ventricle (LV) to body weight (BW) ratios were increased in cardiac HIF-1 α null mice (*f*) despite reduced vascularity. This finding correlated with increased diastolic thickness of the intraventricular septum (IVSd) and the posterior wall (PWd) as determined by echocardiography (*g-h*). The LV end-diastolic diameter (LVEDD) was significantly reduced in HIF-1 α null hearts (*i*), indicating (in conjunction with the wall thickness data) that loss of HIF-1 α leads to thicker hearts with reduced LV chamber size. HIF-1 α null = grey bars; * $P < 0.05$; ** $P < 0.005$.

Fig. 5

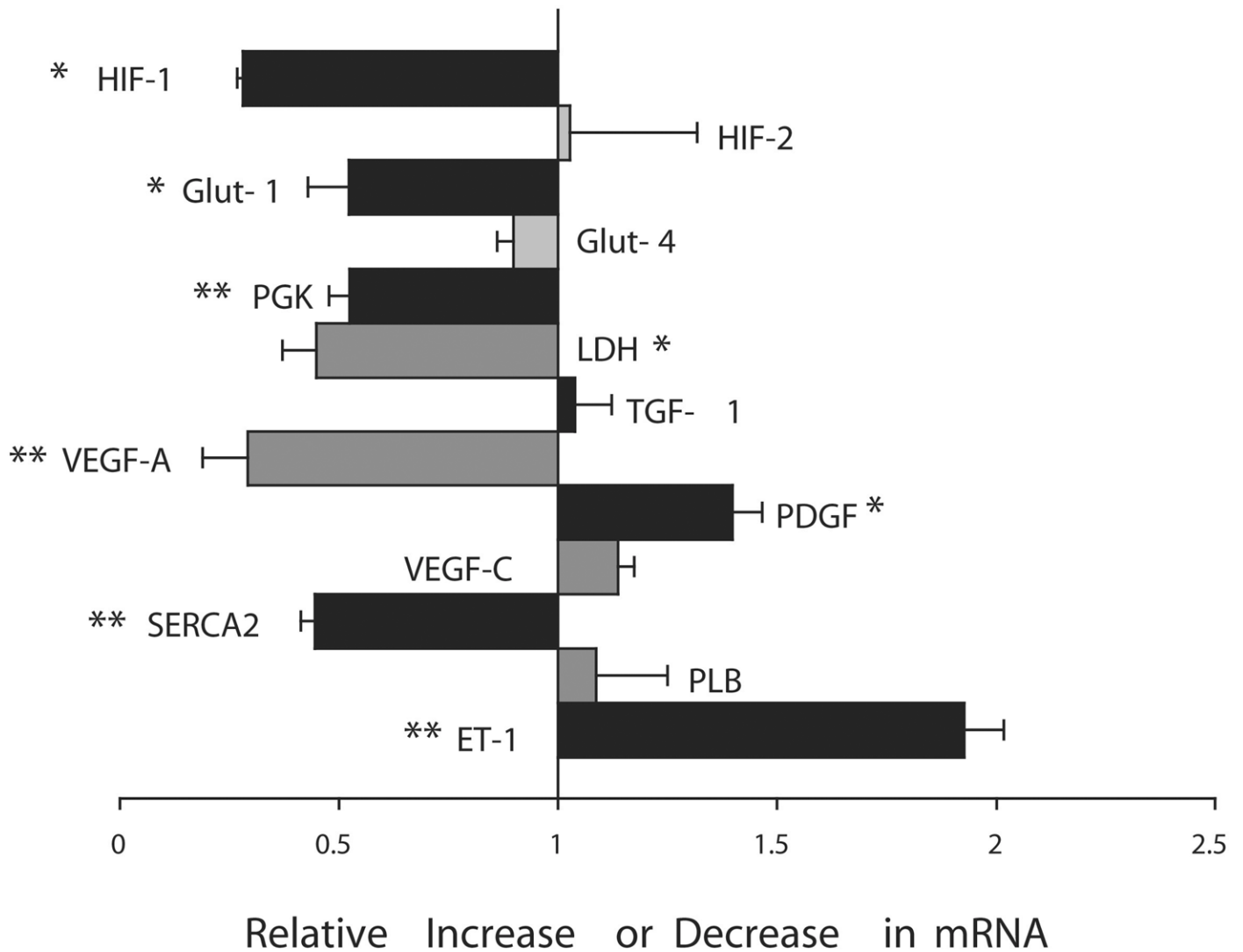


Figure 5. Cardiac myocyte-specific HIF-1 α deletion alters gene expression in the normoxic heart.

DNAase-treated RNA was extracted from the hearts of cardiac HIF1 α null ($n=5$) and age/gender-matched control littermate mice ($n=5$) and relative gene expression quantified by real-time quantitative RT-PCR. Total mRNA for HIF-1 α was reduced to $22.7 \pm 4\%$ of control hearts, and there was no significant compensatory increase in HIF-2 α mRNA. Loss of the HIF-1 α transcription factor specifically in cardiac myocytes resulted in significant reductions in the expression of representative genes involved in angiogenesis, glucose transport, glycolysis, and calcium-handling in cardiac HIF-1 α null hearts, as well as a concomitant increase in endothelin 1 (ET-1) and platelet-derived growth factor B (PDGF-B). VEGF = vascular endothelial growth factor, PGK = phosphoglycerate kinase, LDH = lactate dehydrogenase, Glut = glucose transporter, SERCA2 = sarcoplasmic reticulum calcium ATPase 2a, PLB = phospholamban, TGF- β 1 = transforming growth factor β 1. For all genes, an x -axis value of 1 = identical expression to controls, and all bars represent cardiac HIF-1 α null values relative to control littermates; * $P<0.05$; ** $P<0.005$.

Fig. 6

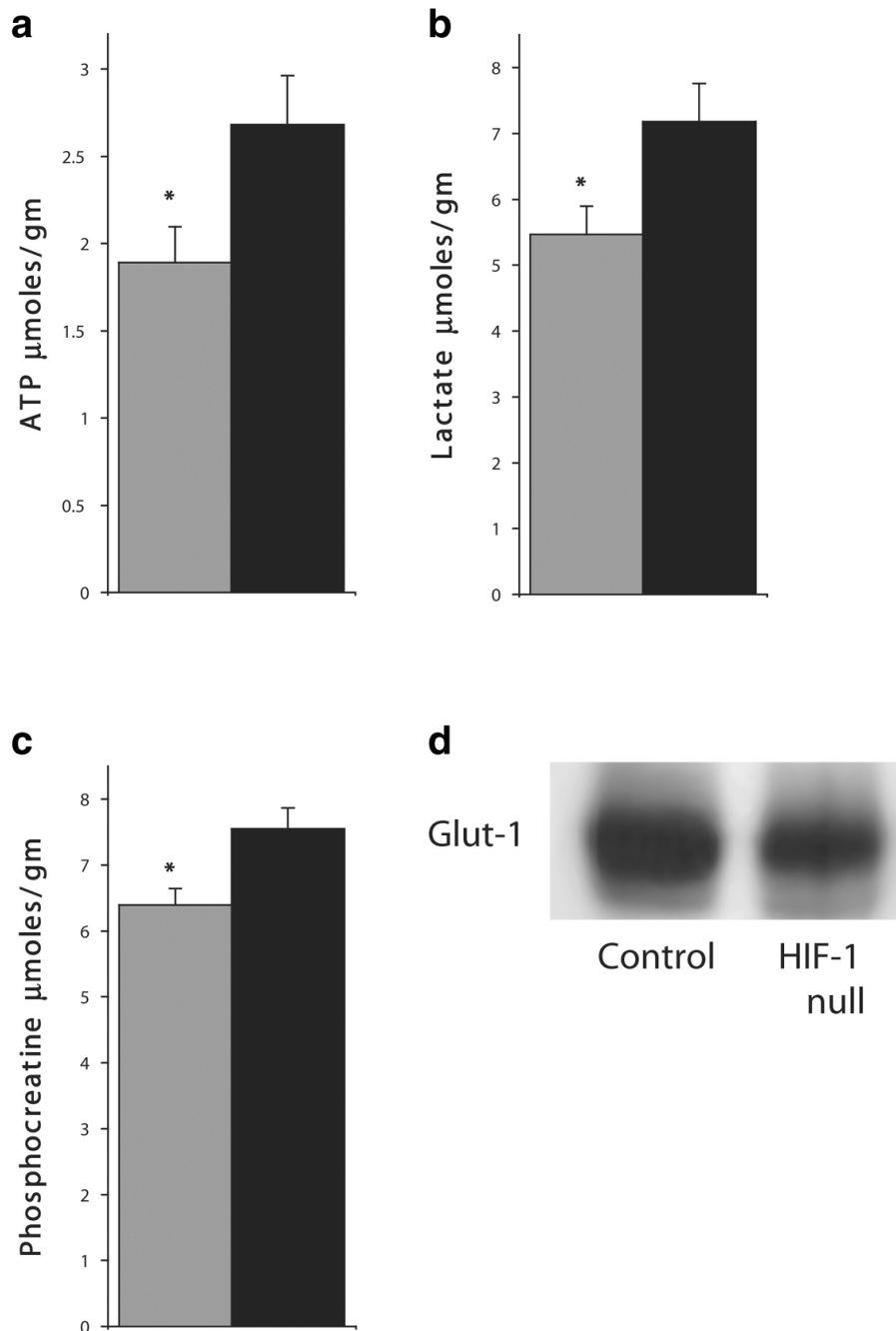


Figure 6. Loss of cardiac myocyte HIF-1 α decreases high-energy phosphate and lactate content in the normoxic heart. **a)** Hearts from cardiac HIF-1 α null and control littermate mice ($n=5/\text{group}$) were rapidly freeze-clamped in situ and used for biochemical determination of ATP content. ATP levels were reduced in HIF-1 α null hearts, as were levels of phosphocreatine (**b**), suggesting an important role for HIF-1 α in determining energy metabolism in the normoxic heart. **c)** Lactate content was also significantly lower in the HIF-1 α null hearts, possibly secondary to the observed reduction in lactate dehydrogenase (LDH) gene expression (see Figure 5). **d)** Glucose transporter Glut-1 protein levels were decreased in cardiac HIF-1 α null hearts, correlating with the observed decrease in Glut-1 mRNA (see Fig. 5); $*P<0.05$.